ACS Photonics

Letter

pubs.acs.org/journal/apchd5

Color Switching with Enhanced Optical Contrast in Ultrathin Phase-Change Materials and Semiconductors Induced by Femtosecond Laser Pulses

Franziska F. Schlich,[†] Peter Zalden,[‡] Aaron M. Lindenberg,[‡] and Ralph Spolenak*[,†]

[†]Laboratory for Nanometallurgy, Department of Materials, ETH Zürich, Vladimir-Prelog-Weg 5, 8093 Zürich, Switzerland

[‡]Stanford Department of Materials Science and Engineering, Stanford University, 476 Lomita Mall, Stanford, California 94305, United States

Supporting Information

ABSTRACT: Ultrathin semiconductors on metals constitute color filters, which selectively absorb wavelength ranges of incident light. This paper demonstrates that these coatings are attractive for tunable color devices by reversibly switching ultrathin phase-change materials on gold between two colors with femtosecond laser pulses. The optical contrast is enhanced compared to conventional thick phase-change materials, and its spectral maximum is tunable via the thickness of the phase-change material. Color switching is even feasible if the phase-change material is replaced by a conventional group IV semiconductor, whose amorphous and crystalline phases are optically less distinct. These structures hold significant promise for optical data storage and for display applications.

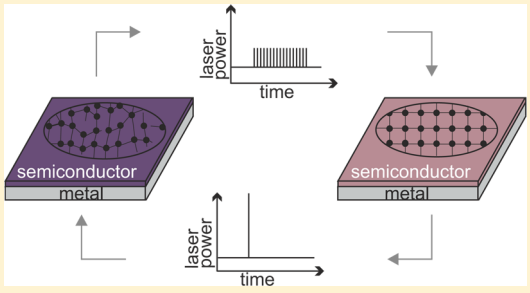

KEYWORDS: *phase-change materials, semiconductors, nanophotonics, color coatings, optical data storage*

Phase-change materials (PCMs) can be switched rapidly and reversibly between the amorphous and the crystalline state associated with a large optical and electrical property contrast.[1] They are applied in optical data storage devices and offer great potential as nonvolatile electronic memories.[2,3] Recently, Hosseini et al. have combined the optical and electronic property modulation of PCMs.[4] They demonstrated electrically induced color changes in phase-change materials ($Ge_2Sb_2Te_5$) with transparent electrodes. The device works analogous to an optical cavity where the thickness of the transparent electrode acts as cavity length. Consequently, the color appearance can be tuned via the thickness of the transparent film. These devices are promising candidates for applications such as ultrafast displays or artificial retina devices.

Here, we present that recently established static color devices[5,6] can be rapidly cycled between two colors: ultrathin semiconductors (5−30 nm) on appropriately chosen[6] highly reflective metals lead to bright color appearances. The large absorption in the semiconductor and the wavelength-dependent phase-shifts at the film interfaces result in absorption resonances; that is, the incident light is selectively absorbed and the reflectance R is strongly attenuated in a small wavelength range whose minimum can be tuned via the thickness of the semiconductor. This effect has been named strong interference and is, for example, used for static color coatings.[5] Here, the strong interference effect is applied to dynamically tunable color devices: The shape of the absorption resonance is strongly dependent on the slope of the imaginary part of the refractive index of the semiconductor.[6] Consequently, only a small change in refractive index results in a large change in reflectivity. We demonstrate that ultrathin phase-change materials and even conventional semiconductors on appropriately chosen metal substrates change color upon a phase transformation. The phase transitions are induced either thermally in a furnace or by femtosecond optical excitation. Conventional semiconductors such as Si typically do not exhibit a strong phase-induced optical contrast compared to phase-change materials.[7] Here, it is shown that the optical contrast of 12 nm thick Si on Ag is comparable to that of PCMs. These findings could lead to a paradigm shift in optical data storage applications: replacing PCMs by conventional semiconductors reduces the costs of production and prevents both the need for toxic materials and the contamination of the processing equipment. Moreover, these layer structures are interesting for nonvolatile, ultrafast display applications.

In Figure 1a, a cross-sectional transmission electron microscope micrograph shows the layer structure of the tunable color device based on $Ge_2Sb_2Te_5$ (GST), as fabricated by magnetron sputter deposition. Au is chosen because its imaginary part of the refractive index k is strongly dependent on the wavelength (see Supporting Information). Only some combinations of the refractive indices of the underlying metal and GST result in an absorption resonance ($R \approx 0$). A large $|dk/d\lambda|$ causes strongly wavelength-dependent refractive indices and results in a smaller wavelength range with ideal combinations of the refractive

Received: October 29, 2014
Published: January 20, 2015

DOI: 10.1021/ph500402r
ACS Photonics 2015, 2, 178−182

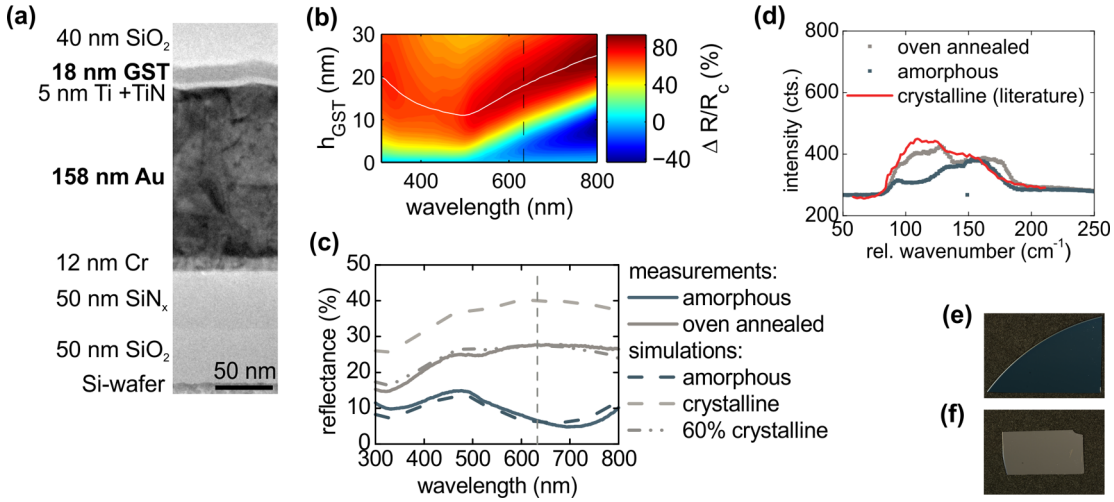

Figure 1. A transmission electron microscopy micrograph (a) of the sample structure is presented. The thickness of GST is optimized in a simulation (b) to maximize the optical contrast between amorphous and crystalline GST at 633 nm wavelength. The white line indicates the maximum optical contrast for each wavelength. The measured and simulated reflectance curves of the amorphous and crystalline sample are shown (c). The colors of the curves correspond to the measured and simulated colors of the samples. For the simulation of the reflectance of the annealed sample we assume that GST is still partly amorphous, as confirmed by Raman spectroscopy measurements (d). The intensity of the Raman spectrum of purely crystalline GST was adapted for a better comparison.[3] Photographs of the as-deposited amorphous (e) and annealed crystalline (f) samples clearly demonstrate the color change from blue to gray upon crystallization.

indices. Therefore, the absorption resonance is narrower and the optical contrast is increased. The SiO_2 capping layer prevents oxidation and evaporation of the phase-change material, and Ti and TiN act as a diffusion barrier between Au and GST. The position of the absorption resonance can be controlled via the thickness (h_{GST}) of GST (see Supporting Information). In simulations h_{GST} is optimized to maximize the reflectance contrast, $(R_c - R_a)/R_c \times 100$, between amorphous and crystalline GST (see Figure 1b). R_c and R_a denote the reflectance in the crystalline and amorphous phase, respectively. The design goal is to optimize the optical contrast at 633 nm wavelength because the reflectivity change upon phase-change is probed for reversible color switching with a continuous laser beam at this wavelength. The maximal optical contrast at 633 nm wavelength $\Delta R/R_c = 85\%$ is achieved for 18 nm thick GST. Figure 1c shows the measured and simulated reflectance spectra of an as-deposited amorphous sample and a crystalline sample annealed at 175 °C for 5 min in a furnace. In the amorphous phase GST exhibits semiconducting behavior, while its crystalline cubic phase is a degenerate semiconductor with orders of magnitude higher carrier concentration.[8] Consequently, an amorphous PCM on top of a metal leads to the strong interference effect and, therefore, a color appearance, while it is metallic gray in the crystalline phase. The measured and simulated reflectance curves of the amorphous layer stack are in excellent agreement. However, the reflectance of the oven-annealed sample is smaller than expected and differs from the simulated spectra. We assume that the majority of the sample crystallized while a small fraction remained amorphous. This is reasonable because for ultrathin PCMs the crystallization temperature and time increase.[9] Consequently, longer annealing or higher annealing temperature would be required for a complete phase transformation. However, here, the annealing time and temperature were minimized to avoid interdiffusion between the different layers. If we include only partial crystallization of GST in the reflectance simulations by assuming that only 60% of the annealed sample crystallized, measurements and simulations are in excellent agreement. The optical contrast at 633 nm is still 77%, exceeding the typically required value for optical data storage of 60%.[10] To prove that the color change is associated with a phase-change, i.e., crystallization, we performed Raman spectroscopy on both samples (see Figure 1d). The Raman peaks of the as-deposited sample at 129 and 152 cm^{-1} are in good agreement with those corresponding to amorphous GST.[3,11] The slightly different Raman peak positions of the annealed sample and that of purely cubic GST confirm the assumption of partly amorphous material in the annealed sample.[3] Figure 1e and f show photographs of an as-deposited amorphous and a crystalline sample. They are clearly distinguishable by their blue and gray color appearance.

For display or data storage applications, fast and reversible color switching is crucial. We demonstrate this by illumination of the sample with femtosecond laser pulses for six switching cycles (see Figure 2a). The reflectance is measured at 633 nm

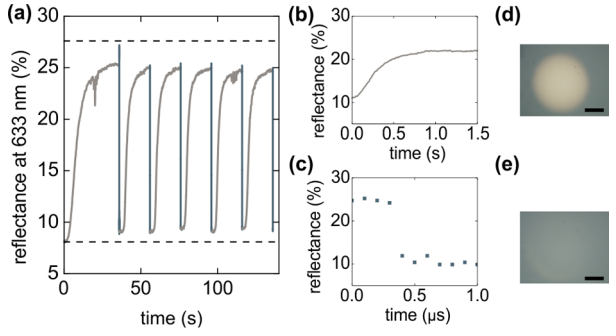

Figure 2. Reversible switching between amorphous and crystalline GST is presented (a). Initialization of the crystallization was performed on a different spot with the same setup parameters and was added to the reversible switching cycles. Crystallization with a 960 Hz repetition rate is shown (b). The time scale of the edge is limited by the experimental resolution (c). The microscope images show crystallized (d) and reamorphized areas (e) of an as-deposited amorphous sample (scale bar: 20 μm).

DOI: 10.1021/ph500402r
ACS Photonics 2015, 2, 178−182

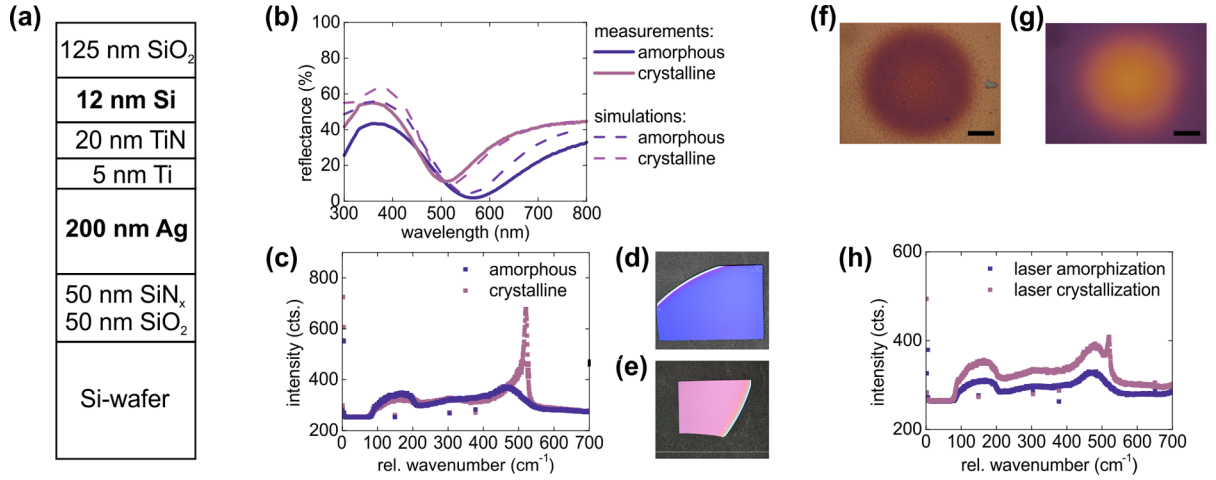

Figure 3. Sample structure (a) of a tunable color device based on ultrathin Si is presented. The reflectance curves (b) of the as-deposited amorphous and annealed crystalline samples were measured and simulated. The colors of the curves correspond to the measured and simulated colors of the samples. The phases of the as-deposited and annealed sample were confirmed by Raman spectroscopy (c). Photographs of the amorphous (d) and crystalline sample (e) prove a strong color change upon crystallization. As a proof of principle the samples were amorphized (f) and crystallized (g) with 60 fs laser pulses. Scale bar: 20 μm. The laser pulse fully amorphized the oven-annealed crystalline Si layer (f), but crystallization of the as-deposited amorphous Si (g) by laser was only partly possible, as indicated by Raman spectroscopy measurements (h).

wavelength. Femtosecond laser pulses were chosen because of two advantages compared to nanosecond pulses: the fluence values are lower due to the absence of thermal loss during the heating process, and the amorphization time is shorter.[12] To amorphize GST, a single pulse of 60 fs at 800 nm is applied with a fluence of 14.3 ± 0.8 mJ cm^{-2}. The crystalline phase is obtained after repetitive excitation at a lower fluence of 4.0 ± 0.3 mJ cm^{-2}. To induce crystallization in the as-deposited amorphous layer, the sample is exposed to 60 fs long pulses for 32 s at a repetition rate of 40 Hz. The phase transformation of as-deposited amorphous GST is limited by nucleation,[2] but recrystallization of a melt-quenched amorphous spot is found to occur faster possibly because of the presence of subcritical crystalline nuclei.[13] Here, the melt-quenched amorphous spot was recrystallized by repetitive illumination for 16 s. Increasing the repetition rate of the laser to 960 Hz (see Figure 2b) reduces the crystallization time to 500 ms. Consequently, in the present case this switching time is limited by the repetition rate of the laser, but it is well known from literature that crystallization can be completed within tens of nanosecond[14] after optical excitation. Figure 2c shows the reflectance change during amorphization. The configuration of the setup limited the determination of the amorphization time to a 100 ns time resolution. The dashed lines in Figure 2a indicate the reflectivity of the as-deposited amorphous and oven-annealed crystalline samples. The reflectance of the laser-amorphized GST is higher than that of the as-deposited sample. This is also visible in Figure 2e. The region that was reamorphized by laser is slightly brighter than the as-deposited amorphous surrounding.

To experimentally verify that only a small change in the refractive index is sufficient for color changes, a sample device with ultrathin Si on Ag was sputter deposited (see Figure 3a). The optical contrast at 633 nm wavelength between amorphous and crystalline Si is increased if the underlying metal Au is replaced by Ag (see also Supporting Information). Narrow absorption resonances and, therefore, bright colors are expected for Si on a metal because the absorption coefficient of Si strongly depends on the wavelength.[6] In Figure 3b, the measured and simulated reflectance spectra of the as-deposited and annealed crystallized sample are presented. The absorption resonance around 570 nm shifts to shorter wavelengths upon phase transformation, and consequently, the optical contrast is largely enhanced. Measurements and simulations are in good agreement, and the small differences could be explained by differences in the refractive indices of the sputtered samples and reference data from the literature. The phases are identified by Raman spectroscopy (see Figure 3c). The amorphous sample has a wide peak at 480 cm^{-1}, and the crystalline phase is characterized by a sharp peak at 520 cm^{-1} which is in good agreement with the literature.[15] The peaks at 150 and 300 cm^{-1} are caused by overtones.[16,17] Photographs of the samples are shown in Figure 3d and e and exhibit clearly distinguishable blue and pink colors. Reversible switching between amorphous and crystalline silicon by laser pulses was already demonstrated in the literature.[18] As a proof of principle, Figure 3f and g demonstrate that laser pulses can induce amorphization and crystallization associated with a color change. The color of the initial crystalline state in image 3f is in good agreement with the laser-induced crystalline spot in image 3g. Color deviations between the microscope images and the photographs can be explained based on differences between the light sources. The material was partly crystallized with 60 fs laser pulses at 800 nm for 1 s at a 960 Hz repetition rate and with a fluence of 18.7 ± 0.7 mJ cm^{-2}. Crystallization of the illuminated spot is verified by Raman measurements, which show a small crystalline peak at 520 cm^{-1} in Figure 3h. A single 60 fs laser pulse with a fluence of 63.8 ± 2.5 mJ cm^{-2} is sufficient to fully amorphize the material, as indicated by the Raman spectrum. Reversible color switching of Si was not feasible, as diffusivities and vapor pressures are high at the melting temperature of Si. For reversible color switching of a standard semiconductor three different approaches are possible:

- Si could be replaced by a semiconductor with lower crystallization and melting temperature, e.g., InSb, GaSb, or Ge.
- A thermal barrier between Si and Ag could be deposited to confine the heat-affected zone to the semiconductor.

DOI: 10.1021/ph500402r
ACS Photonics 2015, 2, 178−182

Here, Al_2O_3, which has a low thermal conductivity, is a possible choice of material.
- Ag could be replaced by a bright metal with high melting temperature such as Cr or Rh.

Replacing Si by InSb is the most promising approach, as the laser power can be strongly reduced for the amorphization cycle, and therefore, ablation and diffusion are less likely.

In conclusion, we introduced a new application for the strong interference effect. Ultrathin phase-change materials and semiconductors on metals can be switched between the amorphous and crystalline phase, associated with a large color change. The reflectance spectra are robust with respect to the angle of incidence of the light.[5,6] This is important for color consistency on flexible substrates or for display applications. The optical contrast of GST integrated in this structure is enhanced, and reversible color switching between blue and gray with femtosecond laser pulses is demonstrated. Besides display applications without power consumption in the static mode, these layered structures are also interesting for applications in optical data storage devices. Pure GST, for example, does not exhibit the required optical contrast for wavelengths around 405 nm and has been replaced by Ge-rich PCMs for third-generation storage media such as Blu-ray disks. In Figure 4, we

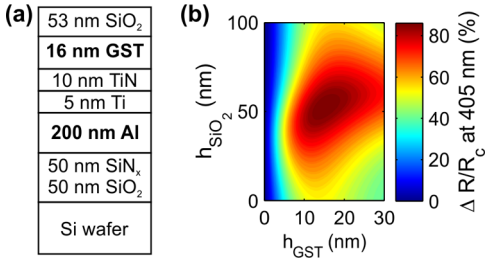

Figure 4. Using a sample structure (a) with ultrathin GST on top of Al and optimizing the thickness of GST and SiO_2 in a simulation (b) can enhance the optical contrast to about 87% at 405 nm wavelength.

demonstrate that optimizing the thickness of GST and SiO_2 on Al results in a sufficiently large optical contrast of more than 87% around 405 nm. Here, Al was chosen as underlying metal, as it results in the largest optical contrast at 405 nm wavelength compared to other highly reflective metals. Consequently, $Ge_2Sb_2Te_5$ can be integrated in a current Blu-ray disk if this layered structure is used. This indicates that a lack of optical contrast, which makes new or sometimes established materials unfavorable for novel optical data storage, may be overcome by exploiting the strong interference effect demonstrated in this paper.

We show that even Si, which is not known for a large optical contrast, can switch between two colors if it is deposited on a metal. Ultrathin Si layers on Ag change from blue to pink upon crystallization with an optical contrast as large as 92% at wavelengths around 572 nm.

To embed these layered structures in optical data storage devices, the crystallization time should be minimized with either longer laser pulses or higher repetition rates. Weidenhof et al., for example, demonstrated crystallization with laser pulses as short as 10 ns, and Cotton et al. showed that employing a femtosecond laser double pulse with an interpulse delay time shorter than 100 ps could trigger partial crystallization of GST.[19,20]

For future reversible color switching, semiconductors with lower melting points and lower diffusion coefficients may prove to be very useful to save energy and simplify the layer architecture.

METHODS

Sample Fabrication. The Cr, Au, Ag, Ti, TiN, and $Ge_2Sb_2Te_5$ layers were deposited by direct current, and the Si and SiO_2 films by alternating current sputter deposition on a (100)-oriented Si substrate with 50 nm SiO_2 and 50 nm SiN_x diffusion barriers. The substrate was rotated at 30 rpm during deposition to achieve uniform film thicknesses, and the base pressure in the chamber exceeded 10^{-6} mbar. To crystallize the layers, the GST sample was annealed at 175 °C for 5 min and the Si sample was annealed at 800 °C for 10 s in a rapid thermal anneal oven.

Reflectance Measurements. The reflectance of the different samples was measured with a fiber spectrometer at an incident angle of 0° and in the wavelength range between 300 and 800 nm.

Photographs. Photographs were taken with a Nikon D7100 camera with a Nikon 200 mm f/4 AF-D macro lens. The samples were illuminated with RB 218N HF lighting units from Kaiser with a color temperature of 5400 K.

Microscope. The microscope images were taken with a Nikon Eclipse L200D optical microscope. The built-in light source was a 12 V/100 W halogen lamp.

Simulations. The reflectance for s-polarized light was simulated with the transfer matrix method described by Pedrotti et al.[21] The refractive indices were taken from the literature.[22−26] The colors of the samples were calculated from the simulated reflectance curves by using the standard illuminant D_{65} and the color matching functions of the 1931 2° standard observer.[27]

Ellipsometry. The refractive index of SiO_2 was measured with an ellipsometer at an incident angle of 70°, and the ellipsometric parameters were fitted with the Cauchy equation.

Raman Spectroscopy. The Raman measurements were performed with a green laser at 532 nm. The laser intensity was reduced to 0.25 mW μm^{-2} for the Si sample and to 0.16 mW μm^{-2} for the GST sample to avoid crystallization of the sample.

Laser Setup. A Ti:sapphire laser illuminated the material with 60 fs laser pulses at 800 nm wavelength. The incident angle was 0°, and the fluence was adjusted with a polarizing beamsplitter for amorphization and crystallization. A HeNe laser at 633 nm wavelength was used to determine the reflectance contrast at the spots. The laser spot diameter of the HeNe laser was 60 μm. The incident angle was 6°, and the reflectivity change was recorded with a photodiode with a temporal resolution of 1 ns. The temporal resolution of the setup is limited by the sampling rate of the oscilloscope in combination with a low-pass filter, which limited the frequency range to 10 MHz and was employed to reduce the impact of high-frequency noise coming from the fast photodiode.

The laser spot diameter of the Ti:sapphire laser was 270 μm for the GST sample and 120 μm for the Si sample.

ASSOCIATED CONTENT

Supporting Information

The influence of the refractive indices of the semiconductor and the metal on the reflectance is explained. Sample structures with different thicknesses of GST and Si are presented. Moreover, the tunable color device introduced here is

DOI: 10.1021/ph500402r
ACS Photonics 2015, 2, 178−182

compared to the device introduced by Hosseini et al. This material is available free of charge via the Internet at http://pubs.acs.org.

AUTHOR INFORMATION

Corresponding Author

*E-mail: ralph.spolenak@mat.ethz.ch.

Notes

The authors declare no competing financial interest.

ACKNOWLEDGMENTS

The authors gratefully acknowledge Andi Wyss' support with the Raman measurements and Diana Courty and Alla Sologubenko for preparing and performing the transmission electron microscopy measurement of the phase-change layer at ScopeM (Scientific Center for Optical and Electron Microscopy) at ETH Zürich. The authors thank the FIRST Center for Micro- and Nanoscience at ETH Zürich for the use of the sputter tool, the optical microscope, the ellipsometer, and the rapid thermal anneal oven. P.Z. acknowledges funding by the Humboldt Foundation, and A.M.L. acknowledges funding by the U.S. Department of Energy, Basic Energy Sciences, Materials Sciences and Engineering Division.

REFERENCES

(1) Welnic, W.; Wuttig, M. Reversible switching in phase-change materials. *Mater. Today* **2008**, *11*, 20−27.

(2) Wuttig, M.; Yamada, N. Phase-change materials for rewriteable data storage. *Nat. Mater.* **2007**, *6*, 824−832.

(3) Kolobov, A. V.; Fons, P.; Frenkel, A. I.; Ankdinov, A. L.; Tominaga, J.; Uruga, T. Understanding the phase-change mechanism of rewritable optical media. *Nat. Mater.* **2004**, *3*, 703−708.

(4) Hosseini, P.; Wright, C. D.; Bhaskaran, H. An optoelectronic framework enabled by low-dimensional phase-change films. *Nature* **2014**, *511*, 206−211.

(5) Kats, M. A.; Blanchard, R.; Genevet, P.; Capasso, F. Nanometre optical coatings based on strong interference effects in highly absorbing media. *Nat. Mater.* **2013**, *12*, 20−24.

(6) Schlich, F. F.; Spolenak, R. Strong interference in ultrathin semiconducting layers on a wide variety of substrate materials. *Appl. Phys. Lett.* **2013**, *103*, 213112-1−213112-4.

(7) Welnic, W.; Botti, S.; Reining, L.; Wuttig, M. Origin of the optical contrast in phase-change materials. *Phys. Rev. Lett.* **2007**, *98*, 236403.

(8) Siegrist, T.; Merkelbach, P.; Wuttig, M. Phase change materials: challenges on the path to a universal storage device. *Annu. Rev. Condens. Matter Phys.* **2012**, *3*, 215−237.

(9) Wei, X.; Shi, L.; Chong, T. C.; Zhao, R.; Lee, H. K. Thickness dependent nano-crystallization in $Ge_2Sb_2Te_5$ films and its effect on devices. *Jpn. J. Appl. Phys.* **2007**, *46*, 2211.

(10) van Pieterson, L.; Lankhorst, M. H. R.; van Schijndel, M.; Kuiper, A. E. T.; Roosen, J. H. J. Phase-change recording materials with a growth-dominated crystallization mechanism: a materials overview. *J. Appl. Phys.* **2005**, *97*, 083520-1−083520-7.

(11) Fu, J.; Shen, X.; Xu, Y.; Wang, G.; Nie, Q.; Lin, C.; Dai, S.; Xu, T.; Wang, R. Structural evolution of $Ge_2Sb_2Te_5$ films under the 488 nm laser irradiation. *Mater. Lett.* **2012**, *88*, 148−151.

(12) Siegel, J.; Gawelda, W.; Puerto, D.; Dorronsoro, C.; Solis, J.; Afonso, C. N.; de Sande, J. C. G.; Bez, R.; Pirovano, A.; Wiemer, C. Amorphization dynamics of $Ge_2Sb_2Te_5$ films upon nano- and femtosecond laser pulse irradiation. *J. Appl. Phys.* **2008**, *103*, 023516-1−023516-7.

(13) Khulbe, P. K.; Wright, E. M.; Mansuripur, M. Crystallization behavior of as-deposited, melt quenched, and primed amorphous states of $Ge_2Sb_{2.3}Te_5$ films. *Appl. Phys. Lett.* **2000**, *88*, 3926−3933.

(14) Siegel, J.; Schropp, A.; Solis, J.; Afonso, C. N.; Wuttig, M. Rewritable phase-change optical recording in $Ge_2Sb_2Te_5$ films induced by picosecond laser pulses. *Appl. Phys. Lett.* **2004**, *84*, 2250−2252.

(15) Houben, L.; Luysberg, M.; Hapke, P.; Carius, R.; Finger, F.; Wagner, H. Structural properties of microcrystalline silicon in the transition from highly crystalline to amorphous growth. *Philos. Mag. A* **1998**, *77*, 1447.

(16) Lockwood, D. J.; Tsybeskov, L. Optical properties of silicon nanocrystal superlattices. *J. Nanophotonics* **2008**, *2*, 1447−1460.

(17) Khayyat, M. M.; Banini, G. K.; Hasko, D. G.; Chaudhri, M. M. Raman microscopy investigations of structural phase transformations in crystalline and amorphous silicon due to indentation with a Vickers diamond at room temperature and at 77 K. *J. Phys. D: Appl. Phys.* **2003**, *36*, 1300.

(18) Sameshima, T.; Usui, S. Pulsed laser-induced amorphization of silicon films. *J. Appl. Phys.* **1991**, *70*, 1281−1289.

(19) Weidenhof, V.; Friedrich, I.; Ziegler, S.; Wuttig, M. Laser induced crystallization of amorphous $Ge_2Sb_2Te_5$ films. *J. Appl. Phys.* **2001**, *89*, 3168−3176.

(20) Cotton, R. L.; Siegel, J. Stimulated crystallization of melt-quenched $Ge_2Sb_2Te_5$ films employing femtosecond laser double pulses. *J. Appl. Phys.* **2012**, *112*, 123520-1−123520-7.

(21) Pedrotti, F. L.; Pedrotti, L. M. In *Introduction to Optics*, 2nd ed.; Prentice-Hall: Englewood Cliffs, NJ, 1993; pp 392, 402.

(22) Johnson, P. B.; Christy, R. W. Optical constants of the noble metals. *Phys. Rev. B* **1972**, *6*, 4370−4379.

(23) Adachi, S.; Takahashi, M. Optical properties of TiN films deposited by direct current reactive sputtering. *J. Appl. Phys.* **2000**, *87*, 1264−1269.

(24) Optical Data from Sopra SA, http://www.sspectra.com/sopra.html, accessed June 2014.

(25) Park, J.-W.; Baek, S. H.; Kang, T. D.; Lee, H.; Kang, Y.-S.; Lee, T.-Y.; Suh, D.-S.; Kim, K. J.; Kim, C. K.; Khang, Y. H.; Da Silva, J. L. F.; Wei, S.-H. Optical properties of (GeTe, Sb_2Te_3) pseudobinary thin films studied with spectroscopic ellipsometry. *Appl. Phys. Lett.* **2008**, *93*, 021914-1−021914-3.

(26) Palik, E. D. In *Handbook of Optical Constants of Solids*; Academic Press: San Diego, CA, 1998; pp 555, 575, 676.

(27) ASTM Standard E308, *Standard Practice for Computing the Colors of Objects by Using the CIE System*; ASTM International: West Conshohocken, PA, 2001.

DOI: 10.1021/ph500402r
ACS Photonics 2015, 2, 178−182